Proceedings of the 9th U.S. National and 10th Canadian Conference on Earthquake Engineering
Compte Rendu de la 9ième Conférence Nationale Américaine et
10ième Conférence Canadienne de Génie Parasismique
July 25-29, 2010, Toronto, Ontario, Canada • Paper No 1221

TRAFFIC LOAD CAPACITY OF A BRIDGE DAMAGED IN AN EARTHQUAKE

V. Terzić[1] and B. Stojadinović[2]

ABSTRACT

Evaluation of the remaining post-earthquake capacity of a bridge to carry self-weight and traffic loads is essential for safe and timely re-opening of the bridge after an earthquake. The post-earthquake truck load capacities of a typical overpass bridge in California are analytically evaluated for a suite of ground motions and set of parameters that have a great influence on the truck load capacity. The paper describes the geometry and analytical model of the bridge, emphasizes the important parameters and shows their influence on the post-earthquake truck load capacity of a bridge. The most influential parameters on the truck load capacity are abutment type, residual drift of the bridge after an earthquake, position of the truck on the bridge relative to the superstructure centerline, and ultimate strain in column reinforcing bars. The analysis has shown that it is unsafe to use the bridge after an earthquake if abutments are not able to provide torsional restraints at the superstructure ends and at least one column fails, meaning that at least one reinforcing bar fractures during the earthquake. If after an earthquake abutments still provide torsional restraints at the superstructure ends, the bridge may be open for traffic immediately after the earthquake if there are not broken reinforcing bars in any of the columns.

Introduction

Although modern highway bridges in California designed using the Caltrans SDC (Caltrans 2006) are expected to maintain at minimum a gravity load-carrying capacity during both frequent and extreme seismic events, as of now, there are no validated, quantitative guidelines for estimating the remaining load carrying capacity of the bridges after an earthquake event. Evaluation of the remaining post-earthquake capacity of a bridge to carry self-weight and traffic loads is essential for safe and timely re-opening of the bridge after an earthquake.

The post-earthquake truck load capacities of a typical overpass bridge in California are analytically evaluated for a suite of ground motions and set of parameters that have a great influence on the truck load capacity. A total of 8 bins of ground motions, each containing 20 records, were utilized. The bins of ground motions distinguish among themselves by the

[1]Doctoral Candidate, Dept. of Civil Engineering, University of California at Berkeley, Berkeley, CA
[2] Professor, Dept. of Civil Engineering, University of California at Berkeley, Berkeley, CA

magnitude of the earthquake, the distance to the fault, the fault type, and presence of directivity effects. Three parameters that influence the truck load capacity: (i) abutment type, (ii) residual drift of the bridge after an earthquake, and (iii) position of the truck on the bridge relative to the superstructure centerline were considered in this study. The analytical model of the bridge used in analysis was calibrated based on the experimental study on the same bridge (Terzic 2009). Although good in capturing lateral displacements and forces of a bridge during an earthquake, the analytical model of the bridge is not capable of capturing residual displacements. Hence, they are simulated by directly applying them after the earthquake simulation was completed. The truck load, located in the critical position on the bridge, is applied next by monotonic increase of the truck weight to induce the failure of the bridge. This way truck load capacity of the bridge was established.

Bridge Model and Loading Regime

The bridge model and loading regime are described in the two subsections. The first subsection gives the details related to bridge geometry, reinforcement, and analytical model of a bridge. The second subsection presents the loading sequences that the bridge was exposed to in the analytical simulations.

Geometry, Reinforcement and Analytical Modeling of the Bridge

Configuration of the bridge used in analytical simulations corresponds to bridge Type 11 in Ketchum et al. (2004). In summary, it is a straight, cast-in-place box girder bridge with five spans and single-column-bents. The bridge has three internal spans of 150’ (45.72 m), two external spans of 120’ (36.58 m), a 39’ (11.9 m) wide deck, and 50’ (15.24 m) tall circular columns 6’- 3” (1.9 m) in diameter. The superstructure is a pre-stressed (CIP/PS) 2-cell box girder supported on neoprene bearing pads under each of the three box webs. Column and deck cross section dimensions are shown in Fig. 1.

Reinforcement of a column consists of longitudinal bars placed around its perimeter and a continuous spiral encasing the longitudinal bars. Each column has 34 longitudinal No.11 (Ø36) reinforcing bars and No.8 (Ø25) spiral with a center to center spacing of 6 inches (0.15 m). Such reinforcement layout gives the longitudinal reinforcement ratio of 1.2% and transverse reinforcement ratio of 0.75%. The cover is 2” (5.1 cm) all around.

The superstructure reinforcement is detailed in Ketchum et al. (2004). In summary, the two-cell box girder contains two layers of longitudinal reinforcing bars in the deck, soffit, and girders, additional mild steel in the deck and soffit over the bents, and post-tensioned steel to provide a 7,000 kips (31,000 kN) pre-stressing force. A cover depth of 1.5 in. (3.8 cm) is used.

To model the bridge, a three-dimensional nonlinear finite element model was developed. It is a spine model of the numerical portion of the bridge structure with line elements located at the centroid of the cross section following the alignment of the bridge (Fig. 2). Three-dimensional beam-column elements with corresponding cross-sectional properties were used to model the superstructure and columns. All six degrees of freedom were restrained at the base of the columns. The PEER Center finite element platform OpenSees (McKenna 1997) was utilized.

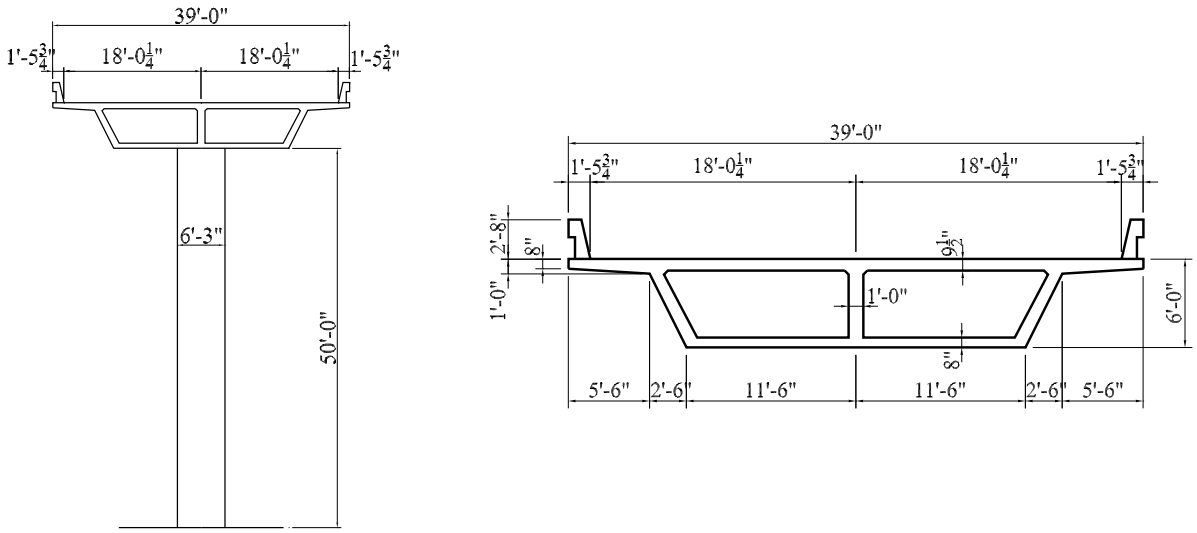

(a) Column cross section (b) Deck cross section

Figure 1. Column and deck cross section of bridge Type 11 (Ketchum et al. 2004).

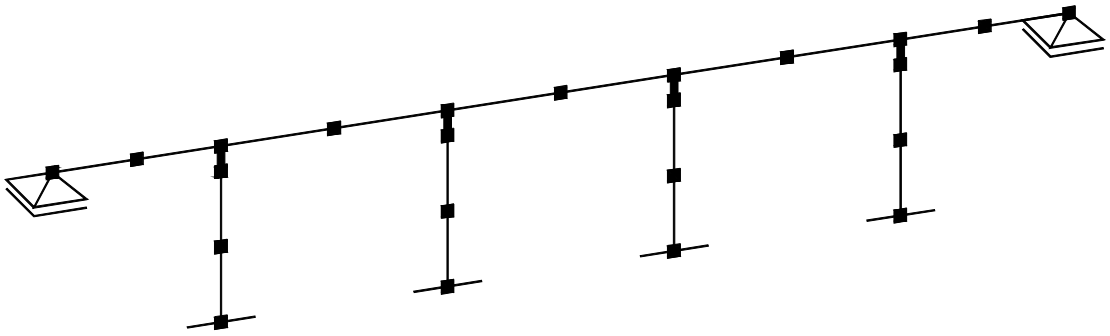

Figure 2. Analytical model of the bridge structure.

The superstructure and columns were modeled with nonlinear beam-column elements that are based on force formulation and consider the spread of plasticity along the element. The element is a line element with integration points at the element ends and along the element length. A fiber cross section, assigned to each integration point, was generated to explicitly account for longitudinal reinforcing bar placement and unconfined and confined concrete effects. Each material in the cross-section had a uniaxial stress-strain relationship assigned to it.

The columns were modeled with two types of elements. The top of the column representing the short portion of the column embedded in the superstructure is modeled as a rigid link. The remainder of the column is modeled with nonlinear beam-column elements. Two elements of equal lengths, each having five integration points, were defined for each column. Integration points along an element were distributed following Gauss-Lobatto integration rule. The fiber section was divided into three parts: reinforcing steel, concrete cover and concrete core, each having a uniaxial stress-strain relationship assigned to it. The reinforcing steel was

modeled by a Giuffre-Menegotto-Pinto uniaxial strain-hardening material model (Menegotto and Pinto, 1973) designated in OpenSees as Steel02. The concrete constitutive models were based on the Kent-Scott-Park model (Kent and Park, 1971) designated in OpenSees as Concrete01. The peak confined concrete strength was determined according to Mander et al. (1988).

Each span of the superstructure was defined with two nonlinear beam-column elements of equal lengths, each having three integration points. Integration points were assigned at element ends and in the middle of the element. Integration weights were 1/6 for end points and 4/6 for the middle point. The constitutive models used for the deck elements are the same as the models used for the column elements. The deck torsional response about its longitudinal axis was assumed to be elasto-plastic with an initial elastic stiffness of GJ/L. A reduction of the torsional moment of inertia (J) is not required since the bridge superstructure is straight and meets the Ordinary Bridge requirements in Section 1.1 of Caltrans SDC (Caltrans 2006). Torsional stress-strain relationship was aggregated with the deck sections at all integration points along the superstructure beam-column elements.

Abutment modeling has a great influence on the post-earthquake truck load capacity of the bridge. Two simple abutment models that generate upper and lower bound of the bridge response for the earthquake and truck load are considered in this study. The actual response of the bridge will lie between these two abutment models. The first abutment model, designated as R_x1, consists of a simple boundary condition module that applies single point constraints against displacement in vertical direction (vertical support) and rotation about the superstructure longitudinal axis (full torsional restraint). The second abutment model, designated as R_x0, applies single point constraint against displacement in vertical direction representing a roller boundary condition at the superstructure end, and no torsional restraint.

To perform dynamic analysis of a bridge all bridge elements had distributed mass assigned along their lengths. Based on distributed mass OpenSees automatically calculates the translational mass of all longitudinal elements in the three global directions of the bridge (longitudinal, transverse, and vertical) and assigns them as lumped masses at each node based on tributary lengths. The rotational mass (mass moment of inertia) for the superstructure is not generated automatically so it was assigned manually at each node. The damping is modeled using Rayleigh damping coefficients that are mass and stiffness proportional. The first two modal periods of the bridge system, assuming the same damping ratio of 3% for both modes, are used to calculate Rayleigh damping coefficients. The effects of column axial loads acting through large lateral displacements, P-Δ effects, are included while analyzing the bridge system. Newmark's time-stepping integration method was used to solve the system of differential equations governing the response of the bridge.

Loading

During an analytical simulation with the purpose of estimating post-earthquake truck load capacity of the bridge, the bridge was exposed to four sequences of loading in the following order: (i) gravity load, (ii) earthquake load, (iii) simulation of residual displacements in the transverse direction of the bridge, and (iv) truck load. The analytical model of the bridge is not capable of capturing residual displacements of the bridge. Hence, after an earthquake they are

simulated in the third loading sequence by applying lateral displacement to the bridge model. The truck load, located in the critical position on the bridge, is applied next by monotonic increase of the truck weight to induce the failure of the bridge. This way the truck load capacity of the bridge was established.

In the process of analytical simulations the bridge was subjected to suites of recorded ground motions. A total of 8 bins, each containing 20 records, were utilized. The bins of ground motions distinguish among themselves by the magnitude of the earthquake, the distance to the fault (near or far), the fault type (strike-slip, reverse), and presence of directivity effects. Every bin of ground motions is adopted from a previous study on structures located in California. Each ground motion record had two orthogonal horizontal components and a vertical acceleration component. The motions were applied uniformly at the base of the structure.

Following an earthquake, all columns were displaced in the transverse direction of the bridge to produce the following drifts: 0.5%, 1%, 1.5%, 2%, 2.5% and 3%; one at a time. The bridge exposed to a far-field earthquake will most likely attain residual drift that is closer to the lower bound of the considered drift range, while the bridge exposed to a near-field earthquake with a strong directivity effect can reach residual drift that is closer to the upper bound of the considered drift range. Following the gravity load and an earthquake, a residual drift was applied to the bridge model up to the magnitude that does not exceed the maximum drift attained during the earthquake.

To simulate the truck load on the bridge standard HS20-44 truck (Caltrans 2004) was used as a typical vehicle. It is a three-axle truck with a fixed spacing of 14 feet (4.3 m) between the first two axles and variable spacing of 14 to 30 feet (4.3 – 9.1 m) between the last two axles. The spacing between the last two axles had to be chosen to produce the maximum stresses in the bridge.

Parametric Study

Parametric study on potentially influential parameters on the post-earthquake truck load capacity of the bridge identified parameters that have a great influence on the truck load capacity (Terzic 2009). The most influential parameters are ultimate strain of reinforcing bars, abutment type, position of the truck on the bridge relative to the superstructure centerline, and residual drift of the bridge after an earthquake.

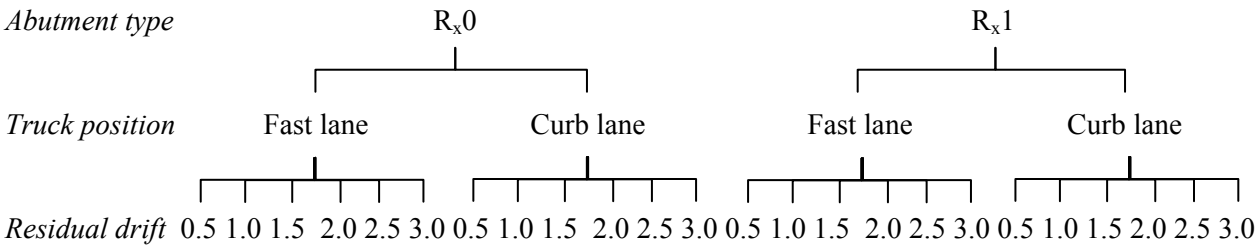

Figure 3. Analysis scheme for one ground motion.

For a fixed value of the ultimate strain of reinforcing bars (defined following recommendation of Caltrans SDC, Caltrans 2006), two abutment types (Rx0 and Rx1), two extreme positions of the truck on the bridge relative to the superstructure centerline (truck in the curb and the fast lane), and six values of the residual drift (0.5%, 1%, 1.5%, 2%, 2.5% and 3%), the total of 24 analyses were performed for each ground motion (Fig. 3).

Truck Load Capacity

Influence of the abutment type, the truck position on the bridge relative to the superstructure centerline, and the residual drift on the truck load capacity of the bridge will be presented hereafter. Since the analytical results relate to the specific bridge, their main purpose is to show the trends and emphasize the parameters that have significant influence on the post-earthquake truck load capacity of a bridge. All results are divided into two groups based on damage that an earthquake causes to the bridge: the first group constitutes those earthquake loading outcomes where the bridge columns did not experience failure; the outcomes where column failure was recorded are in the second group. In this study, failure of a bridge column is defined as fracture of at least one reinforcing bar. Failure of a reinforcing bar is declared when the tension strain in it exceeds 6%, a value defined for the column bar size as the largest usable strain by Caltrans SDC (Caltrans 2006).

None of bridge columns has failed during an earthquake

In the case of earthquakes that do not cause the failure of the bridge columns, truck load capacity does not strongly correlate with the intensity of the ground motion or with the maximum earthquake drift (Terzic 2009). Therefore, the truck load capacity is presented as a function of the residual drift with respect to the abutment type (R_x1 and R_x0) and the position of the truck load relative to the superstructure centerline (Figs. 4 to 7). Mean values of the truck load capacity, along with their ± one standard deviation values ($\pm\sigma$) and ± three standard deviation values ($\pm 3\sigma$), are plotted for different values of residual drifts. To generate the data based on which the mean values of the truck load capacities and their standard deviations can be calculated, the bridge was only analyzed on residual drifts that are smaller than the maximum earthquake drifts. For comparison purposes, the weight of the standard HS20-44 truck is additionally indicated on the plots.

Truck load capacity of the bridge as a function of residual drift degrades faster in the case of the bridge with no torsional restraints at the superstructure ends (R_x0 abutments) than in the case of the bridge with torsional restraints at the superstructure ends (R_x1 abutments). There is an additional reduction of the truck load capacity if the truck is located in the curb lane (maximum eccentricity of the truck load relative to the superstructure centerline) compared to the case when the truck is located in the fast lane (minimum eccentricity of the truck load relative to the superstructure centerline).

In the case of the bridge that has torsional restraints at the superstructure ends (R_x1 abutments) and damaged but not failed columns, a truck equivalent to the standard HS20 truck can use the bridge after an earthquake regardless of its position on the bridge. In the case of the

bridge with no torsional restraints at the superstructure ends (R_x0 abutments) special consideration is necessary if residual drifts are bigger than 1.5% and the bridge is going to be used by a truck with the weight that is at least equivalent to the weight of the standard HS20 truck. However, none of the two considered abutment types is realistic as they generate lower and upper bound for the truck load capacity of the bridge.

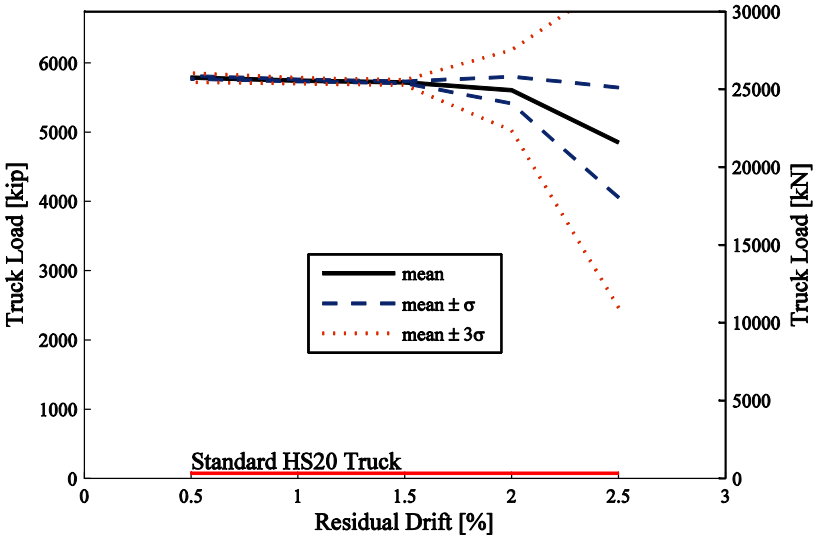

Figure 4. Degradation of the truck load capacity with increase in residual drift for the case of R_x1 abutments when the truck load is in the fast lane.

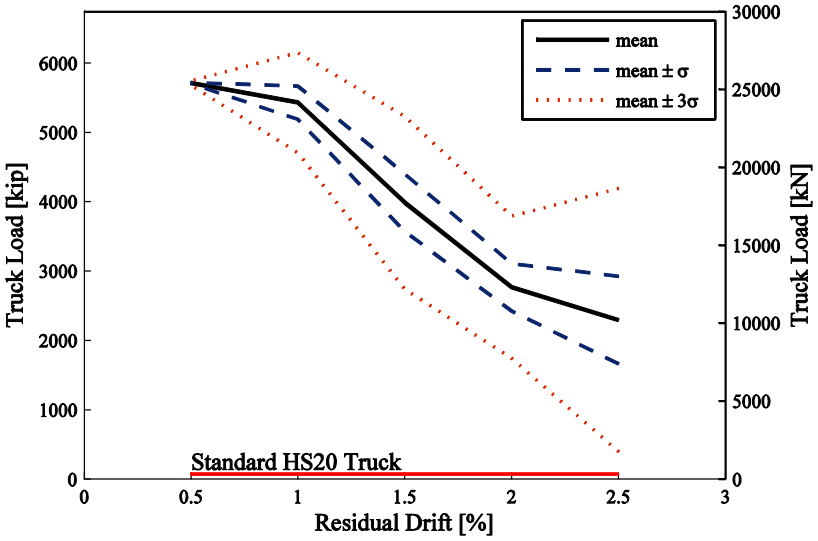

Figure 5. Degradation of the truck load capacity with increase in residual drift for the case of R_x1 abutments when the truck load is in the curb lane.

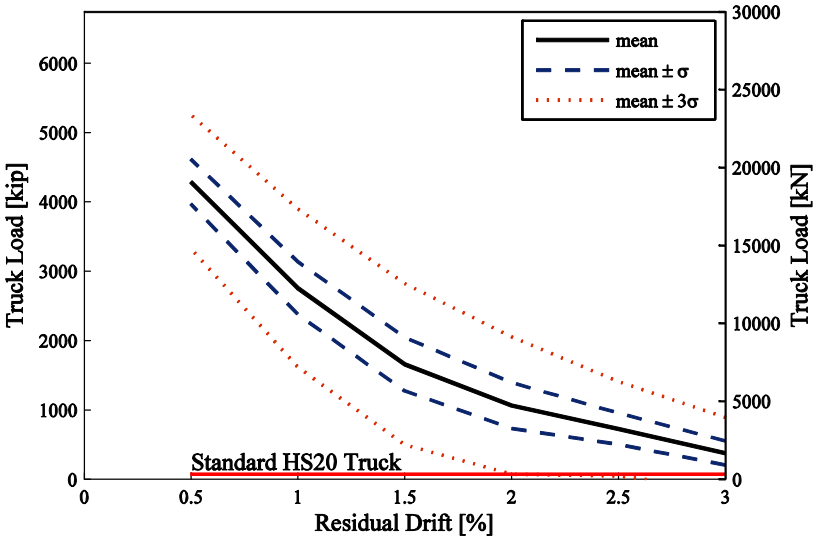

Figure 6. Degradation of the truck load capacity with increase in residual drift for the case of R_x0 abutments when the truck load is in the fast lane.

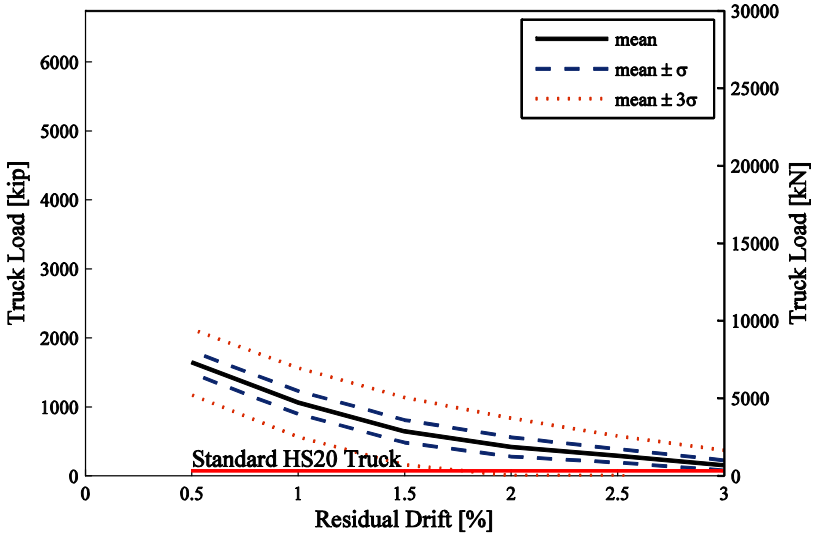

Figure 7. Degradation of the truck load capacity with increase in residual drift for the case of R_x0 abutments when the truck load is in the curb lane.

At least one column has failed during an earthquake

For earthquakes that cause the failure of at least one bridge column, the truck load capacities versus maximum earthquake drifts are plotted for one residual drift, two abutment types and two positions of the truck on the bridge (Fig. 8). Truck load capacity of the bridge for an earthquake that causes the failure of a column and in the case that residual drift does not exceed the maximum earthquake drift is plotted as one point on the graph. The plots additionally contain the level of the weight of the standard HS20-44 truck.

Results presented in Fig. 8 suggest that is not safe to use the bridge after an earthquake if

abutments are not able to provide torsional restraints at the superstructure ends and if at least one reinforcing bar has failed. It is recommended to close the bridge no matter what is the maximum earthquake drift or residual drift. If after an earthquake the abutments still provide torsional restraints at the superstructure ends, the bridge might have some potential for traffic use immediately after the earthquake depending on the damage level of the columns. However, additional investigation is needed to relate post-earthquake truck load capacity of the bridge to the damage level of bridge columns and degree of torsional restraints at the superstructure ends.

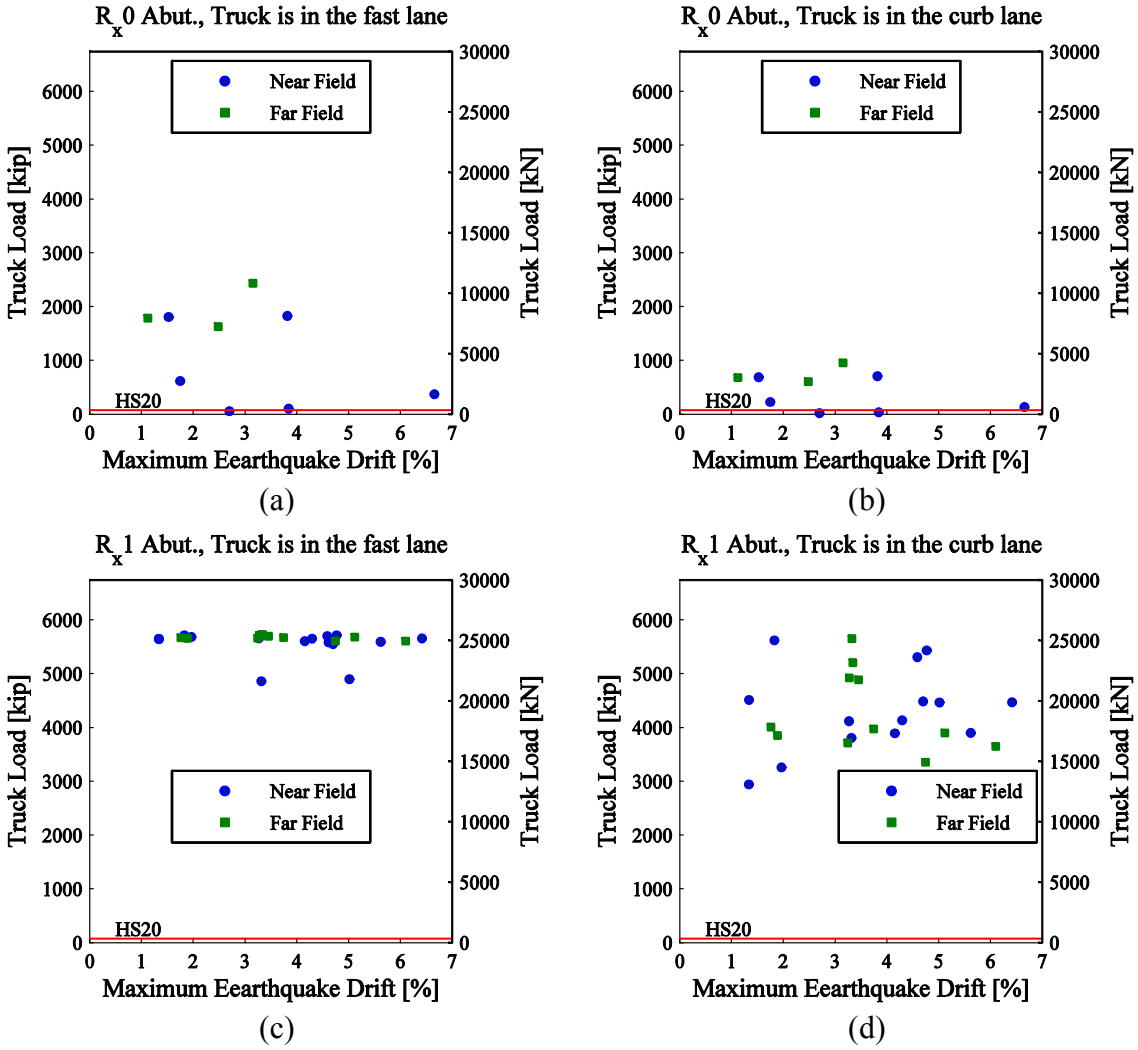

Figure 8. Truck load capacity vs. maximum earthquake drift for the residual drift of 1.0% and the following cases: (a) R_x0 abutment, the truck is in the fast lane; (b) R_x0 abutment, the truck is in the curb lane; (c) R_x1 abutment, the truck is in the fast lane; (d) R_x1 abutment, the truck is in the curb.

Conclusions

Modern highway bridges in California designed using the Caltrans SDC (Caltrans 2006) are expected to maintain at minimum a gravity load-carrying capacity during both frequent and

extreme seismic events. The goal of this study was to provide first-of-its-kind analysis of the remaining load carrying capacity of these bridges after an earthquake. Since the analysis presented herein is related to one specific bridge type, its main purpose is to show the trends of the post-earthquake truck load capacity of that bridge type with the change of significant parameters. As a function of residual drift, the truck load capacity of the bridge degrades faster for the bridge with no torsional restraints at the superstructure ends than for the bridge with torsional restraints at the superstructure ends. There is an additional reduction of the truck load capacity if the truck is located in the curb lane compared to the case when the truck is located in the fast lane. The analysis has also shown that it is unsafe to use the bridge after an earthquake if abutments are not able to provide torsional restraints at the superstructure ends and at least one of the bridge columns has failed, meaning that at least one of its reinforcing bars fractured during the earthquake. In the case of the bridge that has damaged but not failed columns special consideration is necessary if residual drifts are bigger than 1.5%. For this and for other bridge types used in California, additional research is needed to more precisely relate post-earthquake truck load capacity of the bridge to the damage level of bridge columns and degree of torsional restraints at the superstructure ends.

Acknowledgments

This data is based upon work supported by Caltrans project 04-EQ042. This support is gratefully acknowledged. Any opinions, findings, and conclusions or recommendations expressed in this material are those of the authors.

References

Caltrans, 2004. *Bridge Design Specifications*, State of California Department of Transportation.

Caltrans, 2006. *Seismic Design Criteria*, State of California Department of Transportation.

Kent, D. C., and R. Park, 1971. Flexural Members with Confined Concrete, *Journal of Structural Engineering* 97(ST7), 1969-1990.

Ketchum, M., V. Chang, and T. Shantz, 2004. Influence of Design Ground Motion Level on Highway Bridge Costs, *Report PEER 6D01*, University of California, Berkeley.

Mander, J. B., M. J. N. Priestley, and R. Park, 1988. Theoretical Stress-Strain Model for Confined Concrete, *Journal of the Structural Engineering* 114(ST8), 1804-1826.

McKenna, F. T., 1997. Object-oriented finite element programming: frameworks for analysis, algorithms and parallel computing, *Ph.D. Thesis*, University of California, Berkeley.

Menegotto, M., and P. E. Pinto, 1973. Method of analysis for cyclically loaded R/C plane frames including changes in geometry and nonelastic behaviour of elements under combined normal force and bending, *Proc., Symp. on the Resistance and Ultimate Deformability of Structures Acted on by Well Defined Repeated Loads*, IABSE, Zurich, Switzerland, 15–22.

Terzic, V., 2009. Traffic load capacity of a bridge damaged in an earthquake , *Ph.D. Thesis*, University of California, Berkeley.